nuclear fusion
IAEA

PAPER • OPEN ACCESS

Study of ion cyclotron emission excited by tritium ions of fusion products via magnetoacoustic cyclotron instability theory in the EAST

To cite this article: Huapeng Zhang *et al* 2025 *Nucl. Fusion* **65** 076013

OPEN ACCESS
IOP Publishing | International Atomic Energy Agency
Nuclear Fusion
Nucl. Fusion **65** (2025) 076013 (6pp)
https://doi.org/10.1088/1741-4326/addd31

Study of ion cyclotron emission excited by tritium ions of fusion products via magnetoacoustic cyclotron instability theory in the EAST

Huapeng Zhang[1], **Lunan Liu**[2,*], **Wei Zhang**[2,*], **Xuan Sun**[1], **Xinjun Zhang**[2] and **Baolong Hao**[3]

[1] Department of Plasma Physics and Fusion Engineering, School of Nuclear Science and Technology, University of Science and Technology of China, Hefei 230026, China
[2] Institute of Plasma Physics, Chinese Academy of Sciences, Hefei 230031, China
[3] Southwestern Institute of Physics, Chengdu 610041, China

E-mail: liulunan@ipp.ac.cn and wei.zhang@ipp.ac.cn

Received 24 March 2025, revised 7 May 2025
Accepted for publication 27 May 2025
Published 5 June 2025

Abstract

This study investigates the ion cyclotron emission (ICE) excited by tritium ions generated through deuterium−deuterium fusion reactions in the Experimental Advanced Superconducting Tokamak (EAST). ICE is an electromagnetic instability driven by fast ions, and its excitation mechanism is primarily explained by magnetoacoustic cyclotron instability (MCI) theory, which describes energy transfer between fast ions and Alfvénic waves. Since ICE is closely related to the distribution of fast ions, the MCI growth rate is computed using linear theory based on the fast ion distribution calculated by TRANSP. Based on experimental parameters from EAST, we apply MCI theory to analyze the ICE growth rate and investigate the effects of key factors such as the propagation angle and the ratio of fast tritium ions to bulk deuterium plasma density. Experimental findings indicate that ICE excitation is at the fundamental frequency, simulations support that the propagation angle is approximately between 80° and 85°. At the fundamental frequency, the MCI growth rate increases with the propagation angle but decreases as the fast tritium ion density decreases. These results provide insights into the physics of ICE excitation and highlight its potential as the diagnostic tool for fast ions in future fusion reactors, including CFETR, DEMO, and ITER. Understanding ICE can help optimize fusion plasma performance and improve fast-ion confinement in next-generation magnetically confined fusion devices.

Keywords: ion cyclotron emission, magnetoacoustic cyclotron instability, EAST tokamak

(Some figures may appear in colour only in the online journal)

* Authors to whom any correspondence should be addressed.

1. Introduction

Ion cyclotron emission (ICE) is an electromagnetic or electrostatic radiation with frequencies ranging from a few MHz to tens of MHz. It is a collective radiative instability driven by fast ions, commonly observed in magnetically confined plasma, and was the first collective radiative instability driven by confined fusion-born ions detected in JET and TFTR [1–3]. To date, ICE excited by fast ions at both the plasma boundary and the core has been studied in several magnetically confined fusion devices, including Model C [4], TFR [5], KSTAR [6], JET [1, 7], PDX [8], LHD [9, 10], JT-60U [11, 12], DIII-D [13, 14], NSTX [15], NSTX-U [15, 16], TFTR [1], W7-X [17], ASDEX Upgrade [18, 19], TUMAN-3M [20], HL-2A [21], J-TEXT [22], Experimental Advanced Superconducting Tokamak (EAST) [3, 23–26]. Most studies indicate that ICE is closely related to fast ions, which serve as its driving source, and that ICE carries substantial information about fast ion.

ICE can be excited by the non-thermal ion velocity distribution, exhibiting pronounced anisotropy in the pitch angle direction and a bump-on-tail structure (with a positive gradient) in the velocity direction [2, 3, 12, 26]. The magnetoacoustic cyclotron instability (MCI) is a well-established mechanism for ICE excitation, resulting from the resonant interaction between fast magnetoacoustic waves and fast ions. The MCI theory was initially proposed by physicists Belikov and Kolesnichenko in 1975 [27]. Subsequently, Dendy *et al* applied this theory to study ICE excitation in magnetically confined fusion plasma [28]. Currently, the MCI theory is the most widely accepted explanation for ICE excitation.

EAST is equipped with high-power ICRF and NBI systems, delivering a total ICRF power of 12 MW [29] and a total NBI power of 8 MW [30], which establish high-power heating conditions that produce numerous fast ions, potentially inducing ICE. Indeed, we have observed several instances of fast-ion-excited ICE on EAST, including ICE driven by deuterium and tritium ions from deuterium−deuterium fusion [3], i.e. $\mathrm{D} + \mathrm{D} \rightarrow \mathrm{H} + \mathrm{T}$. However, these phenomena have not been comprehensively studied. Consequently, our research primarily utilized the MCI theory to investigate the ICE excited by tritium from deuterium−deuterium fusion, observed in 2023, offering a theoretical interpretation of the ICE phenomenon on EAST.

The structure of this paper is as follows. Section 2 details the diagnostic system and experimental setup. Section 3 presents the theoretical modeling and instability analysis. Section 4 provides a summary.

2. Diagnostic system and experimental setup

EAST is a fully superconducting tokamak with a major radius of $R = 1.85$ m and a minor radius of $a = 0.45$ m [26]. Its objective is to perform experiments under fusion-relevant conditions, emphasizing high-power, long-pulse operations, with a design capability for pulse lengths of up to 1000 s [31].

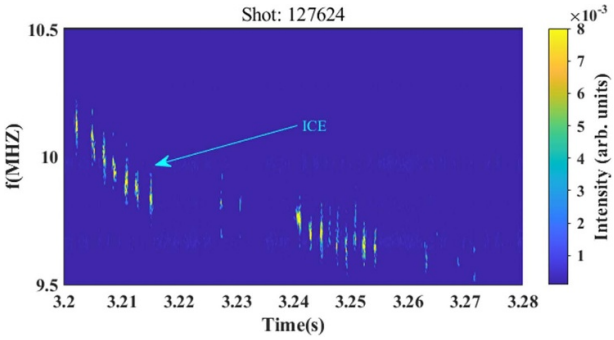

Figure 1. In shot 127 624, from $t = 3.20$ s to $t = 3.28$ s, the ICE frequency spectrum. Reproduced from [3]. The Author(s). © 2025 The Author(s). Published by IOP Publishing Ltd on behalf of the IAEA. CC BY 4.0.

Two ICE probes were installed on EAST to measure ICE. The first type comprises high-frequency B-dot probes (HFBs), positioned on the right side of the ICRF antenna at the I port, with their diagnostic system implemented in 2018 [24, 25]. The second type is an ICRF-antenna-based diagnostic system for ICE detection, installed in 2023 [26]. This probe was initially employed to detect tritium ion-excited ICE from deuterium−deuterium fusion on EAST, with findings reported in 2024 [3]. The correlation spectrum is presented in figure 1. All other physical parameters are detailed in [3].

3. Theoretical modeling and instability analysis

The excitation mechanism for ICE is identified as the MCI, with the core of MCI being the energy transfer between fast ions (in this case, tritium ions) and the fast Alfvénic wave. In certain instances, Bernstein waves may also play a role [32]. The MCI is triggered when tritium ions interact with the fast Alfvénic wave propagating obliquely; resonance occurs when the cyclotron frequency of the ions closely matches that of the magnetic acoustic waves, resulting in instability [19, 33, 34]. The linear analytical theory of the MCI is fundamentally based on Maxwell's equations, which yield the complete dispersion relation of the fast Alfvén wave expressed through dielectric tensor elements. In our study, we employed the following equation to describe the distribution of tritium ions produced by fusion [19, 35]:

$$\mathrm{f_T} = \frac{1}{2\pi^{3/2} u v_r} \exp\left(-\frac{\left(v_\parallel - v_d\right)^2}{v_r^2}\right) \delta\left(v_\perp - u\right). \qquad (1)$$

Here v_r, v_d, and u are constants representing the parallel velocity spread, the average speed, and the unique perpendicular speed of the fast tritium ions, respectively; $v_\parallel$ is the parallel velocity component relative to the local magnetic field with a shifted Gaussian distribution, while $v_\perp$ is the perpendicular velocity component with a delta distribution function. In this study, we consider the boundary distribution of tritium ions generated by deuterium−deuterium fusion in EAST as a ring

distribution. The values of v_r, v_d, and u are determined by the simulation results of TRANSP simulation results, corresponding to the speed at which f_{T} peaks at the plasma edge.

The growth rate γ of obliquely propagating MCI (not parallel to the local magnetic field) is based on previous studies. Using the distribution model of equation (1), the γ is expressed as follows [36, 37]:

$$\gamma = \frac{n_{\mathrm{T}}}{n_{\mathrm{i}}} \frac{\Omega_{\mathrm{i}}^4}{\left[\Omega_{\mathrm{i}} + (\omega - \Omega_{\mathrm{i}}) N_{\|}^2\right]\left[\Omega_{\mathrm{i}} - (\omega + \Omega_{\mathrm{i}}) N_{\|}^2\right]} \times \left(\frac{l\Omega_{\mathrm{T}}}{k_{\|} v_r} M_l - \frac{2u_{\perp}^2}{v_{\mathrm{r}}^2} \eta_l N_l\right) \frac{\sqrt{\pi}}{2\omega} \mathrm{e}^{-\eta_l^2}. \quad (2)$$

Here, the ratio of fast tritium ions (n_{T}) to bulk deuterium plasma number density $\xi_{\mathrm{T}} = \frac{n_{\mathrm{T}}}{n_{\mathrm{i}}}$ represents the number density ratio, Ω denotes ion cyclotron frequency, ω refers to wave frequency, and the subscripts i and T signify bulk deuterium ions and tritium ions produced by deuterium and deuterium fusion, respectively. Additionally $N_{\|} = k_{\|} c_A/\omega$, where $k_{\|}$ is the parallel wavenumber, c_{A} is the Alfvénic speed, $\eta_l = \left(\omega - k_{\|} v_d - l\Omega_{\mathrm{T}}\right)/k_{\|} v_r$, and l is a positive integer. The expressions for M_l and N_l in the equation are provided below [36]:

$$\mathrm{M}_l = 2l\frac{\omega}{\Omega_i}\left(J_l'^2 + \frac{1}{\mathrm{z}_T^2}\left(l^2 - \mathrm{z}_T^2\right) J_l^2\right) - 2\frac{\omega^2 - \Omega_i^2}{\Omega_i^2}\frac{J_l J_l'}{\mathrm{z}_T} \times \left[l^2 \mathrm{N}_{\perp}^2 - \left(\mathrm{z}_T^2 - 2l^2\right)\mathrm{N}_{\|}^2\right] + \frac{2J_l J_l'}{\mathrm{z}_T}\left(\mathrm{z}_T^2 - 2l^2\right)$$

$$\mathrm{N}_l = -2l\frac{\omega}{\Omega_i}\frac{J_l J_l'}{\mathrm{z}_T} + \frac{\omega^2 - \Omega_i^2}{\Omega_i^2}\left[N_{\|}^2\left(\frac{l^2 J_l^2}{\mathrm{z}_T^2} + J_l'^2\right) + \mathrm{N}_{\perp}^2\frac{l^2 J_l^2}{\mathrm{z}_T^2}\right] + \frac{l^2 J_l^2}{\mathrm{z}_T^2} + J_l'^2. \quad (3)$$

Here, J_l is the Bessel function, J_l' is its first-order derivative, $z_T = k_{\perp} u/\Omega_{\mathrm{T}}$, $k_{\perp}$ denotes the perpendicular wavenumber, and $N_{\perp} = k_{\perp} c_A/\omega$. The frequency of the fast Alfvénic wave is as follows [37]:

$$\omega^2 = \frac{1}{2} c_{\mathrm{A}}^2 \left[k^2 + k_{\|}^2 + k^2 k_{\|}^2 \frac{c_{\mathrm{A}}^2}{\Omega_{\mathrm{i}}^2} + \sqrt{\left(k^2 + k_{\|}^2 + k^2 k_{\|}^2 \frac{c_{\mathrm{A}}^2}{\Omega_{\mathrm{i}}^2}\right)^2 - 4k^2 k_{\|}^2}\right]. \quad (4)$$

In this dispersion relation, $k^2 = k_{\perp} + k_{\|}^2$; using this relation, the parallel wavenumber is calculated as $k_{\|} = k \times \cos\theta$ and the perpendicular wavenumber as $k_{\perp} = k \times \sin\theta$, where θ is the angle between the wave and the local magnetic field (propagation angle). When the instability growth rate γ is greater than 0 (i.e. positive), it indicates instability. According to McClements *et al* N_l is generally positive and ensures $\gamma > 0$ only when $\eta_l < 0$, implying $\omega - k_{\|} v_d < l\Omega_{\mathrm{T}}$, while M_l is generally negative, depending on the values of the parameters l and z_T.

Near the plasma boundary $R = 2.29$ m on EAST, the velocity of the fast tritium ion produced by the deuterium−deuterium fusion reaction is smaller than the Alfvénic speed c_{A}. To investigate the instability of MCI, we first treat these quantities as constants. The distribution function in pitch-energy space for shot 127 624 at 3.2 s, representing tritium ions generated by the deuterium−deuterium fusion reaction at the plasma boundary on the low-field side of EAST, is depicted in figure 2. This distribution, derived from TRANSP simulations using the NUBEAM and FUSION modules [38–40], is considered a steady-state distribution during the onset of ICE. The pitch angle is predominantly centered around 0.65, as indicated by the solid red line. The energies of the fast tritium ions corresponding to half the maximum value of the distribution function, defined as 1/2 f_{max}, are denoted as E_{max} and E_{min}. We extracted the fast tritium ion distribution function near the angle of 0.65 from the distribution function shown in figure 2 to calculate the constant v_r, as shown in figure 3. Then, we determine the individual constants based on figures 2 and 3 and assigned numerical

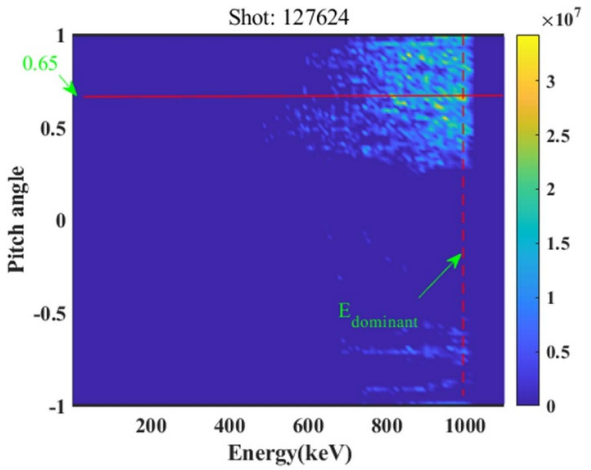

Figure 2. Distribution of fast tritium ions from TRANSP simulations at the plasma edge near $R = 2.29$ m.

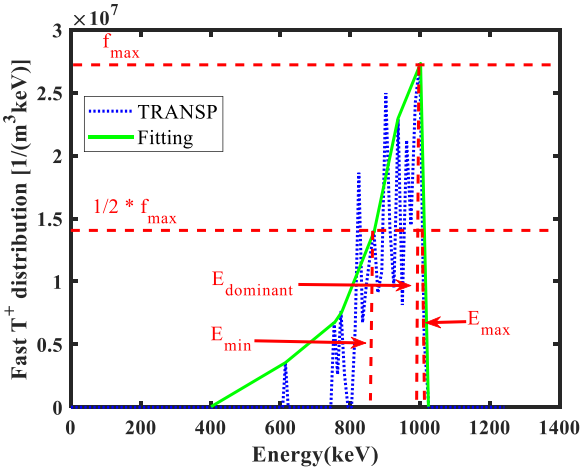

Figure 3. TRANSP calculated fast tritium ions energy distribution with a specific pitch value $\rho = 0.65$. f_{max} represents the most prominent distribution function of fast tritium ions.

values of other physical quantities. From figure 3, the energy of E_{dominant} at $f_{\max}$ is 999.302 keV, the energy of $E_{\max}$ at 1/2 $f_{\max}$ is 1012.17 keV, and $E_{\min}$ at 1/2 $f_{\max}$ is 869.355 keV. Using the following equations,

$$v_r = \sqrt{\frac{2E_{\max}}{m_{\mathrm{T}}} - \frac{2E_{\min}}{m_{\mathrm{T}}}},\ v_d = \sqrt{\frac{2E_{\text{dominant}}}{m_{\mathrm{T}}}} \times \text{pitch angle}$$
$$u = \sqrt{\frac{2E_{\text{dominant}}}{m\mathrm{T}} - v_d^2} \tag{5}$$

we obtained the values for the parallel velocity spread v_r, the average speed v_d and the unique perpendicular speed u of the fast tritium ions in the formula m_{T} is the mass of the fusion product tritium ion in this study.

According to the simulation results of TRANSP, other parameters can also be calculated. Here the ratio of fast tritium ions (n_{T}) to bulk deuterium plasma number density ξ_{T} is approximately 2.0×10^{-5}. Additionally, as the parallel wavenumber and fast Alfvénic wave were not measured in this experiment, we selected a nearly perpendicular propagation angle, $\theta = 80°$, based on prior studies. With all required parameters provided—derived from assumptions, experimental data, and simulated calculations—we chose l = 1,2,3,4, representing the fundamental frequency, second harmonic, third harmonic, and fourth harmonic of the ICE, respectively. We then calculated the MCI growth rate γ using equation (2), treating γ as a function of $\omega - k_{\|} v_d$. Figure 4 illustrates how γ varies with $\omega - k_{\|} v_d$; the MCI growth rate γ at the fundamental frequency is about 2.1×10^3, the largest within the scope of our study, and the γ value at the higher harmonic is smaller. To examine the dependence of γ of MCI on the propagation angle θ and number density ξ_{T}, we evaluated these factors separately. For the fundamental frequency (near Ω_{T}, the cyclotron frequency of the fusion-product tritium ion), second harmonic, third harmonic, and fourth harmonic of the ICE, while keeping other parameters constant, we selected wave propagation angles $\theta = 70°$, $75°$, $85°$ and compared them with $\theta = 80°$. The results are presented in figure 5. Within our study's range, the MCI growth rate γ increases as the propagation angle approaches perpendicularity; at $\theta = 85°$, γ is approximately 4.6×10^3. Figure 5 also shows that the growth rate near a propagation angle of 80° aligns with the power maximum of the ICE fundamental frequency, suggesting that ICE propagates at an angle close to 80°. Finally, we investigated the effect of number density ξ_{T} on γ for MCI in the context of ICE. We selected three values—$\xi_{\mathrm{T}} = 7.0\times10^{-6}$, 2.0×10^{-6}, 7.0×10^{-7} —and compared them with the experimental and TRANSP-simulated case of $\xi_{\mathrm{T}} = 2.0\times10^{-5}$. The γ value of MCI decreases with lower ξ_T and the relevant results are shown in figure 6, yet even a minimal presence of fast ions can excite sufficiently strong ICE.

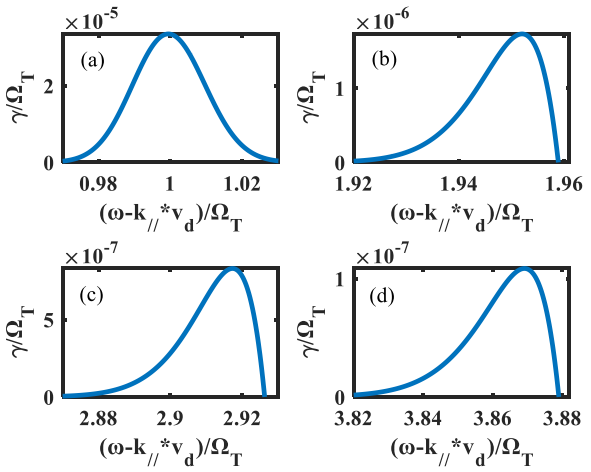

Figure 4. MCI growth rate γ as a function of $\omega - k_{\|} v_d$ at different frequencies, (*a*) $l = 1$, the fundamental frequency, (*b*) $l = 2$, second harmonic frequency, (*c*) $l = 3$, third harmonic frequency, (*d*) $l = 4$, fourth harmonic frequency.

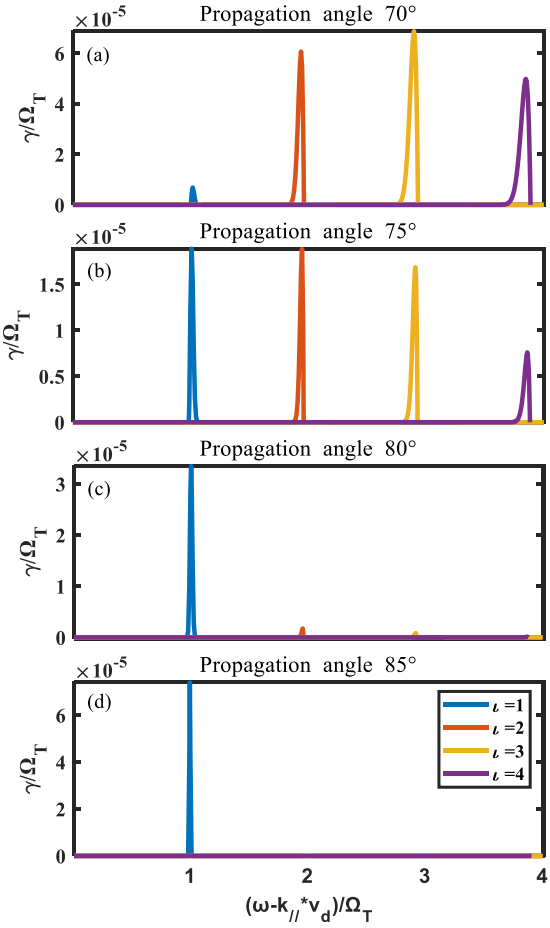

Figure 5. MCI growth rate γ as a function of $\omega - k_{\|} v_d$ at different propagation angles θ at l = 1,2,3,4, including (*a*) is $\theta = 70°$, (*b*) is $\theta = 75°$, (*c*) is $\theta = 80°$, and (*d*) is $\theta = 85°$.

4. Consistency between simulation and experimental results

We systematically compared simulation results based on the theory of MCI with experimentally observed ICE signals from the EAST tokamak. Regarding instability growth rates, numerical simulations demonstrate maximum growth occurring at the fundamental cyclotron frequency under typical experimental parameters, which explains the highest intensity

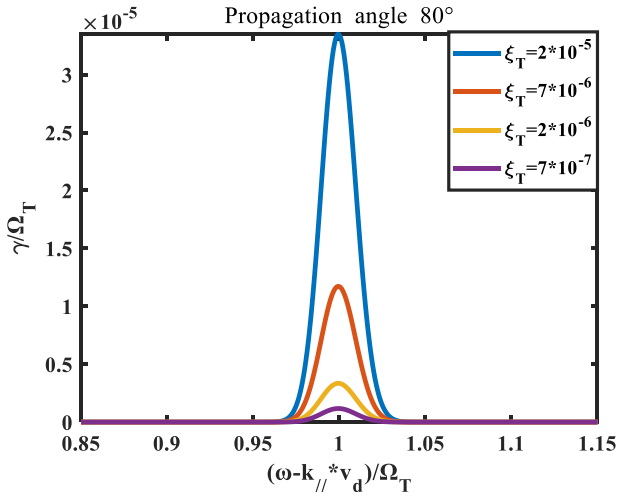

Figure 6. MCI growth rate γ as a function of $\omega - k_{\|} v_d$ at different number density $\xi_{\mathrm{T}} = \frac{n_{\mathrm{T}}}{n_{\mathrm{i}}}$.

observed in this frequency band. Conversely, slower growth at higher harmonics corresponds to weaker radiation intensity—a trend likewise reflected in experimental measurements.

The simulations further reveal spatial distribution characteristics of ICE. Due to the coupling between wave propagation properties and nonuniform ion distribution, theoretical analysis predicts stronger ICE excitation at the plasma edge. This prediction is supported by signal intensity profiles obtained from external magnetic probes in EAST. Future studies will incorporate refined velocity distribution functions and nonlinear evolution effects to further improve model accuracy.

Our observed ICE characteristics are similar with the ICE reported by Cauffman *et al* in the TFTR device [41]. The simulation results are similar with the findings of Ochoukov and Liu *et al* [19, 33], demonstrating consistently higher instability growth rates γ at spectral peaks—at the fundamental cyclotron frequency or its harmonics (where ICE intensities are maximized). This correlation further support the MCI mechanism as the dominant driver.

In summary, the simulations exhibit strong consistency with experimental data in both harmonic features and intensity distribution, confirming the validity of the MCI mechanism for interpreting ICE phenomena in EAST experiments.

5. Summary

This study presents the investigation of the MCI growth rate γ, the excitation mechanism for ICE driven by tritium ions produced from deuterium−deuterium fusion reactions on EAST. Using experimental parameters, we show that ICE is most effectively excited at the fundamental frequency of ICE. The distribution of fast tritium ions was obtained through TRANSP simulations, based on the distribution, the growth rate of the MCI was calculated using the theory of MCI. We examine the influence of the propagation angle θ and the ratio of fast tritium ions to bulk deuterium plasma number density ($\xi_{\mathrm{T}} = \frac{n_{\mathrm{T}}}{n_{\mathrm{i}}}$) on MCI excitation. Our findings indicate that, for the studied range, larger propagation angles enhance ICE excitation at the fundamental frequency. Higher harmonic emission weakens as propagation angle increases. These results match well with experimental observations. It is also noted that whereas lower fast ions densities reduce its likelihood. Investigating MCI advances our understanding of ICE physics.

Acknowledgments

This work is supported by the Strategic Priority Research Program of the Chinese Academy of Sciences (Grant No. XDB0790303), the National Natural Science Foundation under Grant No. 12175226, and National Natural Science Foundation of China under Grant Nos. 12175273, 12105184, 11975265, National magnetic confinement fusion energy development research project under Grant Nos. 2022YFE03190200, 2019YFE03070000, the Comprehensive Research Facility for Fusion Technology Program of China under Contract No. 2018-000052-73-01001228. And this work uses the TRANSP code, which is funded by Princeton Plasma Physics Laboratory/Princeton University under Contract Number DE-AC02-09CH11466 with the U.S. Department of Energy. The United States Government retains and the publisher, by accepting the article/presentation for publication, acknowledges that the United States Government retains a non-exclusive, paid-up, irrevocable, world-wide license to publish or reproduce the published form of this manuscript, or allow others to do so, for United States Government purpose.

ORCID iDs

Huapeng Zhang https://orcid.org/0009-0009-9172-2984
Lunan Liu https://orcid.org/0000-0001-5694-7031
Wei Zhang https://orcid.org/0000-0002-5951-6779
Xuan Sun https://orcid.org/0000-0002-8338-3654
Xinjun Zhang https://orcid.org/0000-0002-8717-354X
Baolong Hao https://orcid.org/0000-0003-3009-0660

References

[1] Dendy R.O. and McClements K.G. 2015 *Plasma Phys. Control. Fusion* **57** 044002
[2] Dendy R.O., McClements K.G., Lashmore-Davies C.N., Cottrell G.A., Majeski R. and Cauffman S. 1995 *Nucl. Fusion* **35** 1733–42
[3] Zhang H.P. *et al* 2025 *Nucl. Fusion* **65** 026057
[4] Brown I.G., Rothman M.A. and Sinclair R.M. 1968 *Bull. Am. Phys. Soc.* **13** 280
[5] Amano C. and Inoue M. 1978 *Rev. Sci. Instrum.* **49** 208
[6] Thatipamula S.G., Yun G.S., Leem J., Park H.K., Kim K.W., Akiyama T. and Lee S.G. 2016 *Plasma Phys. Control. Fusion* **58** 065003
[7] McClements K.G., Hunt C., Dendy R.O. and Cottrell G.A. 1999 *Phys. Rev. Lett.* **82** 2099

[8] Bhadra D.K., Chiu S.C., Buchenauer D. and Hwang D. 1986 *Nucl. Fusion* **26** 201
[9] Saito K. *et al* 2013 *Plasma Sci. Technol.* **15** 209
[10] Saito K. *et al* 2009 *Fusion Eng. Des.* **84** 1676
[11] Ichimura M., Higaki H., Kakimoto S., Yamaguchi Y., Nemoto K., Katano M., Ishikawa M., Moriyama S. and Suzuki T. 2008 *Nucl. Fusion* **48** 035012
[12] Sumida S., Shinohara K., Ikezoe R., Ichimura M., Sakamoto M., Hirata M. and Ide S. 2019 *Plasma Phys. Control. Fusion* **61** 025014
[13] Thome K.E., Pace D.C., Pinsker R.I., Van Zeeland M.A., Heidbrink W.W. and Austin M.E. 2019 *Nucl. Fusion* **59** 086011
[14] DeGrandchamp G.H., Lestz J.B., Van Zeeland M.A., Du X.D., Heidbrink W.W., Thome K.E., Crocker N.A. and Pinsker R.I. 2022 *Nucl. Fusion* **62** 106033
[15] Fredrickson E.D., Gorelenkov N.N., Bell R.E., Diallo A., LeBlanc B.P. and Podestà M. 2019 *Phys. Plasmas* **26** 032111
[16] Fredrickson E.D., Gorelenkov N.N., Bell R.E., Diallo A., LeBlanc B.P., Lestz J. and Podestà M. (NSTX Team) 2021 *Nucl. Fusion* **61** 086007
[17] Moseev D. *et al* 2021 *Rev. Sci. Instrum.* **92** 033546
[18] Ochoukov R. *et al* 2020 *Nucl. Fusion* **60** 126043
[19] Liu L.N. *et al* 2021 *Nucl. Fusion* **61** 026004
[20] Askinazi L.G., Belokurov A.A., Gin D.B., Kornev V.A., Lebedev S.V., Shevelev A.E., Tukachinsky A.S. and Zhubr N.A. 2018 *Nucl. Fusion* **58** 082003
[21] Liu L.Z. *et al* 2023 *Nucl. Fusion* **63** 104004
[22] Zou G. *et al* 2024 *Fusion Eng. Des.* **203** 114457
[23] Liu L.N. *et al* 2020 *Nucl. Fusion* **60** 044002
[24] Liu L.N. *et al* 2019 *Rev. Sci. Instrum.* **90** 063504
[25] Liu L.N., Zhang X., Qin C., Zhao Y., Yuan S., Mao Y. and Wang J. 2019 *J. Plasma Phys.* **85** 905850214
[26] Zhang H.P. *et al* 2024 *Rev. Sci. Instrum.* **95** 053504
[27] Belikov V.S. and Kolesnichenko Ya I. 1976 *Sov. Phys. Tech. Phys.* **20** 1146–51
[28] Dendy R.O., Lashmore-Davies C.N. and Kam K.F. 1992 *Phys. Fluids B* **4** 3996–4006
[29] Zhang X.J. *et al* 2022 *Nucl. Fusion* **62** 086038
[30] Xie Y.H. *et al* 2022 *IEEE Trans. Plasma Sci.* **50** 4086
[31] Hu J., Xi W. and Zhang J. 2023 *AAPPS Bull.* **33** 8
[32] Dendy R.O. 1994 *Plasma Phys. Control. Fusion* **36** 163
[33] Ochoukov R. *et al* 2019 *Nucl. Fusion* **59** 086032
[34] Kong H.Z., Xie H. and Sun J. 2023 *Nucl. Fusion* **63** 126034
[35] Moseev D. and Salewski M. 2019 *Phys. Plasmas* **26** 020901
[36] McClements K.G., Dendy R.O., Lashmore-Davies C.N., Cottrell G.A., Cauffman S. and Majeski R. 1996 *Phys. Plasmas* **3** 543–53
[37] Dendy R.O., Lashmore-Davies C.N., McClements K.G. and Cottrell G.A. 1994 *Phys. Plasmas* **1** 1918–28
[38] Pankin A Y, Breslau J, Gorelenkova M, Andre R, Grierson B, Sachdev J, Goliyad M and Perumpilly G 2025 TRANSP integrated modeling code for interpretive and predictive analysis of tokamak plasmas (arXiv:2406.07781)
[39] Hawryluk R.J. 1980 An empirical approach to tokamak transport *Physics of Plasmas Close to Thermonuclear Conditions* vol 1, ed B. Coppi *et al* (CEC) pp 19–46
[40] Pankin A., McCune D., Andre R., Bateman G. and Kritz A. 2004 *Comput. Phys. Commun.* **159** 157–84
[41] Cauffman S. *et al* 1995 *Nucl. Fusion* **35** 1597–602